Available online at www.sciencedirect.com
ScienceDirect
Trans. Nonferrous Met. Soc. China 25(2015) 973−980
Transactions of Nonferrous Metals Society of China
www.tnmsc.cn

Response surface optimization of process parameters for removal of F and Cl from zinc oxide fume by microwave roasting

Zhi-qiang LI[1,2,3,4,5], Jing LI[1,2,3,4,5], Li-bo ZHANG[1,2,3,4,5], Jin-hui PENG[1,2,3,4,5], Shi-xing WANG[1,2,3,4,5], Ai-yuan MA[1,2,3,4,5], Bao-bao WANG[1,2,3,4,5]

1. Yunnan Provincial Key Laboratory of Intensification Metallurgy, Kunming University of Science and Technology, Kunming 650093, China;
2. National Local Joint Laboratory of Engineering Application of Microwave Energy and Equipment Technology, Kunming University of Science and Technology, Kunming 650093, China;
3. Key Laboratory of Unconventional Metallurgy, Ministry of Education, Kunming University of Science and Technology, Kunming 650093, China;
4. State International Joint Research Center of Advanced Preparation Technology of Superhard Materials, Kunming University of Science and Technology, Kunming 650093, China;
5. Faculty of Metallurgy and Energy Engineering, Kunming University of Science and Technology, Kunming 650093, China

Received 16 April 2014; accepted 13 July 2014

Abstract: Microwave was applied to roasting the zinc oxide fume obtained from fuming furnace for the removal of F and Cl. The effects of important parameters, such as roasting temperature, holding time and stirring speed, were investigated and the process conditions were optimized using response surface methodology (RSM). The results show that the effects of roasting temperature and holding time on the removal rate of F and Cl are the most significant, and the effect of stirring speed is the second. The defluorination rate reaches 92.6% while the dechlorination rate reaches 90.2%, under the process conditions of roasting temperature of 700 °C, holding time of 80 min and stirring speed of 120 r/min. The results indicate that the removal of F and Cl from fuming furnace production of zinc oxide fumes using microwave roasting process is feasible and reliable.

Key words: zinc oxide fume; F; Cl; removal rate; microwave roasting; response surface methodology

1 Introduction

The recovery of useful materials and metals from various secondary sources is of paramount importance due to economic and environmental benefits. Zinc oxide fume generated from fuming furnace contains significant amounts of Zn and Pb along with a small amount of valuable metals such as Ge, Ga, In, Cd and Ag [1−4]. Additionally, zinc oxide fume has different levels of F and Cl, which strongly affects its utilization in the subsequent Zn-based electrical products [5,6]. F and Cl concentrations in electrolytes must meet electrolysis requirements (ρ(F)<80 mg/L, ρ(Cl)<100 mg/L) in the zinc electrolysis process [7,8]. Currently, there are two popular pretreatment processes for the removal of F and Cl, namely pyrometallurgical roasting and caustic washing. The removal rates of high F and Cl concentrations in multiple hearth furnaces, rotary kilns, and other conventional roasting approaches are low, while removal via caustic washing results in the generation of large amounts of waste water, which demand subsequent waste water treatment system [9,10]. This necessitates development of better processes for removal of F and Cl.

Microwave metallurgy is successfully adopted for microwave drying, microwave-assisted grinding, microwave-assisted reduction, and microwave strengthening leaching [11−13], which fully demonstrates microwave metallurgy as a highly efficient,

Foundation item: Project (51104073) supported by the National Natural Science Foundation of China; Project (2013AA064003) supported by the High-tech Research and Development Program of China; Project (2014CB643404) supported by the National Basic Research Program of China; Project (2012HB008) supported by Yunnan Province Young Academic Technology Leader Reserve Talents, China
Corresponding author: Li-bo ZHANG; Tel: +86-871-65138997; E-mail: libozhang77@163.com
DOI: 10.1016/S1003-6326(15)63687-1

clean, and green metallurgy technology [14,15]. The uniqueness of microwave heating can be attributed to a short processing time, selective and volumetric heating, and controllable heating process. Compared with the traditional heating style, the material with high-loss factor is heated preferentially by microwave, and a phase interface is created with large temperature gradient. Phase interface cracks are generated, which strengthen phase separation. The microwave absorbance of chloride and sulfide is strong, while that of ZnO and PbO is weak in the zinc oxide fume [16]. Based on the selective heating property of microwave, the separation of impurities (F and Cl) as volatile components will be strengthened, as a result, the contents of F and Cl in the leaching solution could meet the electrolysis process requirements.

In the present work, the removal of F and Cl from zinc oxide dust by microwave roasting was investigated. The roasting temperature, holding time and stirring speed were selected as three influencing factors, and the removal rate was the response. Response surface methodology (RSM) based on the central composite design (CCD) was employed to determine the optimal conditions and a quadratic model correlating the removal of F and Cl to three variables was then developed.

2 Experimental

2.1 Materials

The zinc oxide fume used in the experiments was received from a fuming furnace smelting process in Yunnan Province, China, which was the mixture of filter bag fume and surface cooler fume with mass ratio of 7:3. The main chemical compositions of the zinc oxide dust are listed in Table 1.

Table 1 Chemical compositions of zinc oxide dust sample (mass fraction, %)

Zn	Pb	Ge	Cd	Fe	Sb
53.17	22.38	0.048	0.21	0.38	0.23
S	As	F	Cl	SiO_2	CaO
3.84	1.04	0.0874	0.0783	0.65	0.096

Table 1 reveals that the zinc oxide fume contains high Zn and Pb. The F and Cl in the zinc oxide fume may be incorporated into the leaching solution, thus resulting in excessive F and Cl concentrations, causing lots of problems in the zinc electrolysis process.

2.2 Mechanism

Compared with the conventional heating, microwave can achieve rapid heating. The traditional heating is based on conventional heat transfer mode from the exterior to the interior driven by the temperature gradient, while the heating mode through microwave heating is based on the dielectric loss of the zinc oxide fume and selective heating of molecules or atoms. Thus, the in-situ energy conversion can be realized by rapidly heating with the energy accumulation in the micro-region with high energy density, which can greatly reduce the roasting time of zinc oxide fume.

In addition, the microwave absorbance of Cl and F existing in zinc oxide fume is stronger than that of ZnO and PbO in the zinc oxide fume [16], which provides the possibility for strengthening the separating effect of F and Cl in volatile components. With the preferred heating of Cl and F, the separation of impurities (F and Cl) as volatile components can be strengthened.

2.3 Experimental set-up and procedures

The main experimental equipment is a power of 3 kW box-type microwave reactor(2450 MHz) designed by Key Laboratory of Unconventional Metallurgy, Ministry of Education, Kunming University of Science and Technology, China. The schematic experimental set-up is shown in Fig. 1.

To carry out the experiment, 300 g sample was dried, ground and placed into the mullite crucible firstly, and then transferred to the microwave reactor, which could realize continuously adjustable and automatic temperature control. Secondly, the starting of the experiment was marked by activating the microwave, stirring, and off-gas absorption systems. The stirring system facilitates the reaction enabling the release of F

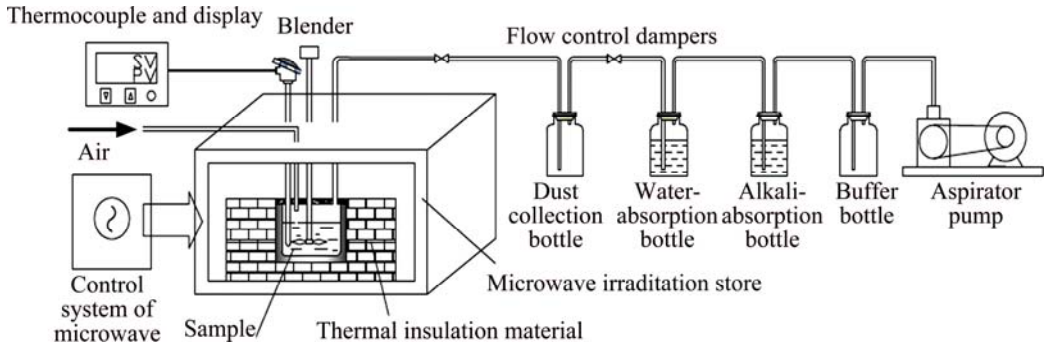

Fig. 1 Connection diagram of microwave roasting experimental equipment

and Cl components. Thirdly, air was passed into the reactor after the material was heated to the set roasting temperature. Air flow rate was controlled by the air into system which consists of a rotameter and a mini air compressor pump. The samples after microwave roasting for a given time were cooled to room temperature.

The F and Cl contents of the samples were estimated using fluorine ion selective electrode and silver chloride turbidimetric method, respectively [17,18]. The raw materials were measured to contain 166.3 mg/L F and 145.4 mg/L Cl. The removal rate (η) was mathematically expressed as

$$\eta = \frac{w - w'}{w} \times 100\% \quad (1)$$

where w and w' represent the contents in the initial materials and samples after roasting for F and Cl, respectively.

2.4 Analysis method

Based on previous works, three influencing factors, namely the roasting temperature (X_1, °C), holding time (X_2, min), and stirring speed (X_3, r/min) were considered independent variables. The dependent variables were the F and Cl removal rates of zinc oxide dust (Y_1, Y_2, %). Table 2 shows the independent variables, experimental range and levels of the design model. In order to describe the nature of the response surface in the optimum region, a central composite design with three coded levels was performed. In general, central composite designs need a total of (2^k+2k+N_0) runs, where k is the number of studied factors, 2^k is the points from the factorial design, $2k$ is the face-centered points and N_0 is the number of experiments carried out at the centre.

Table 2 Experimental range and level of variables

Level code	Roasting temperature, X_1/°C	Holding time, X_2/min	Stirring speed, X_3/(r·min^{-1})
−1	600	60	100
0	700	80	120
1	800	100	140

3 Results and discussion

3.1 Response analysis and interpretation

A total of 20 runs of the CCD experiment responses are shown in Table 3. Each group of the experiment was repeated twice, the average rate was employed. Considering the operability of experiments, roasting experiments, the roasting temperatures of runs 9 and 10 were set as 532 and 868 °C, the holding time of runs 11 and 12 as 46 and 114 min, and the stirring speeds of runs 13 and 14 as 86 and 154 r/min, respectively. The

Table 3 Central composite design arrangement and results

Run	Roasting temperature, X_1/°C	Holding time, X_2/min	Stirring speed, X_3/(r·min^{-1})	Defluorination rate, Y_1/%	Dechlorination rate, Y_2/%
1	600	60	100	65.5	58.4
2	800	60	100	87.4	83.1
3	600	100	100	75.1	69.7
4	800	100	100	93.0	91.4
5	600	60	140	68.3	62.6
6	800	60	140	89.2	87.5
7	600	100	140	78.8	72.5
8	800	100	140	94.6	93.3
9	532	80	120	55.3	48.0
10	868	80	120	87.9	86.7
11	700	46	120	76.8	65.3
12	700	114	120	94.1	92.0
13	700	80	86	87.8	84.9
14	700	80	154	93.7	92.5
15	700	80	120	91.8	91.0
16	700	80	120	92.0	90.5
17	700	80	120	92.5	90.9
18	700	80	120	91.8	91.0
19	700	80	120	90.7	89.6
20	700	80	120	93.0	90.2

defluorination rate of zinc oxide dust varied from 65.5% to 94.6% while the dechlorination rate varied from 58.4% to 93.3%.

The ANOVA results of the quadratic model for the defluorination and dechlorination rates are listed in Tables 4 and 5, respectively. The model *F*-values of 257.66 and 87.75 imply that the model is significant. There is only a 0.01% chance that *F*-value of this large model could occur by chance. Values of "Prob.>*F*" of less than 0.050 indicate that the model terms are significant [19]. In this case, X_1, X_2, X_3, X_1^2 and X_2^2 are the significant model terms. According to MYERS et al [19], for a good fitness of a model, the correlation coefficient should be at least 0.80. The "Pred *R*-squared" of 0.9957 (R_1^2) is in reasonable agreement with the "Adj *R*-squared" of 0.9918 ($R_{1\,adj}^2$) listed in Table 4. The "Pred *R*-squared" of 0.9875 (R_2^2) is in reasonable agreement with the "Adj *R*-squared" of 0.9762($R_{2\,adj}^2$) listed in Table 5. Hence, the model can be used to navigate the design space.

Table 4 Defluorination rate analysis of variance for response surface quadratic model

Source	Sum of square	d*f*	Mean square	*F*-value	*P*-value
Model	2383.15	9	264.79	257.66	<0.0001
X_1	1262.86	1	1262.86	1228.85	<0.0001
X_2	265.32	1	265.32	258.18	<0.0001
X_3	28.77	1	28.77	28.00	0.0004
X_1X_2	10.35	1	10.35	10.07	0.0699
X_1X_3	1.20	1	1.20	1.17	0.3050
X_2X_3	0.06	1	0.06	0.06	0.8121
X_1^2	771.26	1	771.26	750.49	< 0.0001
X_2^2	84.32	1	84.32	82.05	< 0.0001
X_3^2	4.28	1	4.28	4.17	0.0685
Residual	10.28	10	1.03	–	–

R_1^2=0.9957, $R_{1\,adj}^2$=0.9918

Table 5 Dechlorination rate analysis of variance for response surface quadratic model

Source	Sum of square	d*f*	Mean square	*F*-value	*P*-value
Model	3488.34	9	387.59	87.75	< 0.0001
X_1	1809.15	1	1809.15	409.60	< 0.0001
X_2	471.02	1	471.02	106.64	< 0.0001
X_3	49.81	1	49.81	11.28	0.0073
X_1X_2	6.30	1	6.30	1.43	0.2599
X_1X_3	0.06	1	0.06	0.01	0.9086
X_2X_3	1.90	1	1.90	0.43	0.5266
X_1^2	976.93	1	976.93	221.18	< 0.0001
X_2^2	258.87	1	258.87	58.61	< 0.0001
X_3^2	6.76	1	6.76	1.53	0.2442
Residual	44.17	10	4.42	–	–

R_2^2=0.9875, $R_{2\,adj}^2$=0.9762

The constants and coefficients were obtained by fitting the data listed in Tables 4 and 5 into Eqs. (2) and (3), respectively:

$$Y_1=-464.47+1.19X_1+1.56X_2+0.52X_3-5.69\times10^{-4}X_1X_2-1.94\times10^{-4}X_1X_3+2.18\times10^{-3}X_2X_3-7.32\times10^{-4}X_1^2-6.05\times10^{-3}X_2^2-1.36\times10^{-3}X_3^2 \quad (2)$$

$$Y_2=-561.11+1.30X_1+2.45X_2+0.63X_3-4.44\times10^{-4}X_1X_2-4.38\times10^{-5}X_1X_3-1.2\times10^{-3}X_2X_3-8.23\times10^{-4}X_1^2-0.011X_2^2-1.71\times10^{-3}X_3^2 \quad (3)$$

It is important to confirm that the selected model provides an adequate approximation to the real system. By using the diagnostic plots, including normal probability vs studentized residuals and the predicted vs actual value, the model adequacy can be judged [19,20].

Figure 2 shows the normal probability plots of the studentized residuals for the initial discharge capacity. The normal probability plot indicates that the residuals follow a normal distribution, and the points follow a straight line, verifying that the model is valid and plausibly fits the experimental data.

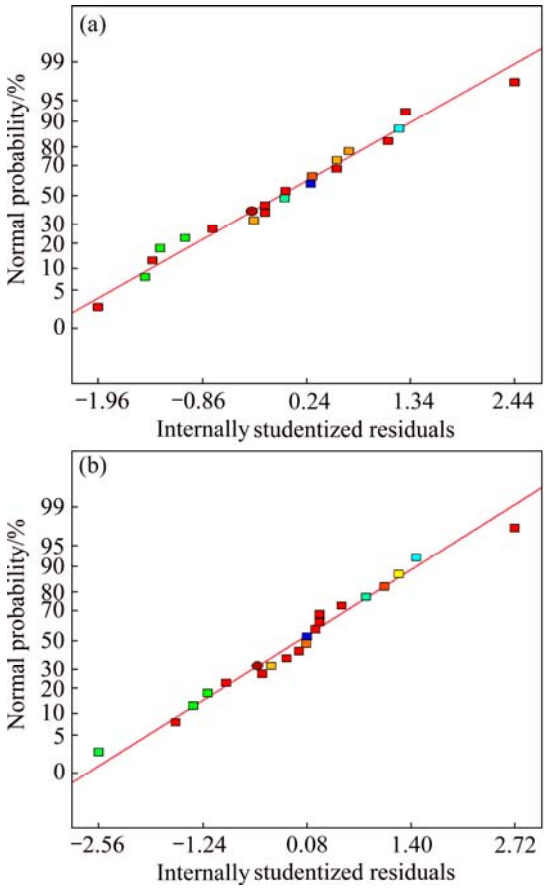

Fig. 2 Normal probability plots of internally studentized residuals: (a) Defluorination rate; (b) Dechlorination rate

As seen in Fig. 3, the actual response values are the experimental data for a particular run, and the predicted response values are evaluated by the approximating functions. The predicted values are in good agreement with the experimental values, indicating that the model is valid and successfully fits the experimental data.

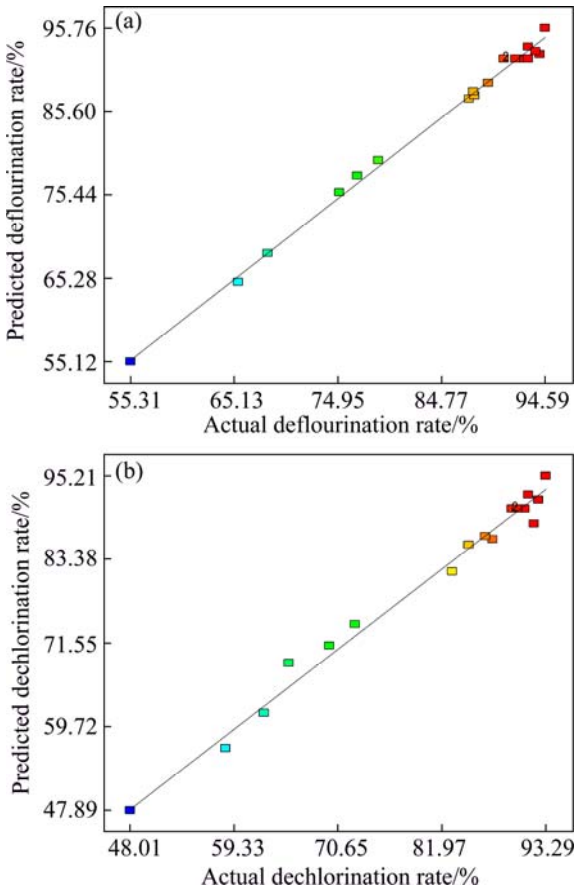

Fig. 3 Linear correlation between actual and predicted rates: (a) Defluorination rate; (b) Dechlorination rate

3.2 Response surface

To achieve better understanding of the interactions of the variables and to determine the optimum level of each variable for the maximum dechlorination rate of zinc oxide dust, three-dimensional response surface plots of the relationship between X_1 and X_2, X_1 and X_3, X_2 and X_3 are calculated and illustrated in Fig. 4. The values of X_1, X_2 and X_3 were held constant at their average values. The figures were constructed to assess the interactive relationships between the independent variables and the response.

Figures 4 (a) and (d) show the defluorination and dechlorination rates of zinc oxide dust as a function of the roasting temperature and holding time when the stirring speed keeps constant at 120 r/min. The roasting temperature has a more significant positive effect on defluorination and dechlorination rates than the holding time. The rate increases quickly as the roasting temperature increases before 700 °C and then becomes smooth. This can be easily explained by the fact that halide vapor pressure increases rapidly with the temperature rising before 700 °C. And the higher the vapor pressure and evaporation rate are, the higher the defluorination and dechlorination rates will be. However, the rate only slightly increases when roasting temperature increases to 700 °C. The samples will be sintered at an excessive temperature, which affects the diffusion of chlorides from the solids into the gas, seriously. Compared with roasting temperature, the holding time has a smaller effect on defluorination and dechlorination rates.

Figure 5 shows the SEM image of zinc oxide fume. It can be found that two different phases (the white phase and the gray phase) exist in the zinc oxide fume. To further explore the distribution characteristics of F and Cl, an EDS line scan (Fig. 6) was applied. On the micro-regions, Zn was aggregated in the gray phase, F, Cl, Pb and S were enriched in the white phase while O was scattered over. The better microwave absorbance of halides will be taken full use to selectively heat the aggregation of halides and strengthen the separation of halides as volatile components. The XRD pattern of raw sample (Fig. 7) shows that Pb and S combined in PbS phase. PbS phase with good microwave absorbance [16] was preferentially heated, which provided better conditions for heating the fluorides and chlorides of the same micro-region rapidly. Thus, microwave roasting could realize higher F and Cl removal rates at a lower roasting temperature compared with the conventional roasting.

In addition, XRD patterns of raw material and roasted sample are shown in Fig. 7. The peak of PbS phase in the roasted sample disappeared, which indicated that PbS was oxidized to PbO. The oxidation reaction of PbS is exothermic, which further strengthened the separation of halides in the same micro-region.

As shown in Figs. 4(b) and (e), the defluorination and dechlorination rates increased with the increase of the stirring speed. This can be easily explained by the fact that the defluorination and dechlorination rates were controlled by the diffusion at a certain temperature. The reaction interface increased with increasing the stirring speed and a larger solid−gas interface improved the defluorination and dechlorination rates significantly. But compared with roasting temperature, the stirring speed had a smaller effect on the defluorination and dechlorination rates, which indicated that the stirring speed had a weaker effect on the rate.

Figures 4(c) and (f) show the effect of the holding time and the stirring speed on the defluorination and dechlorination rates at a constant roasting temperature. The defluorination and dechlorination rates increased

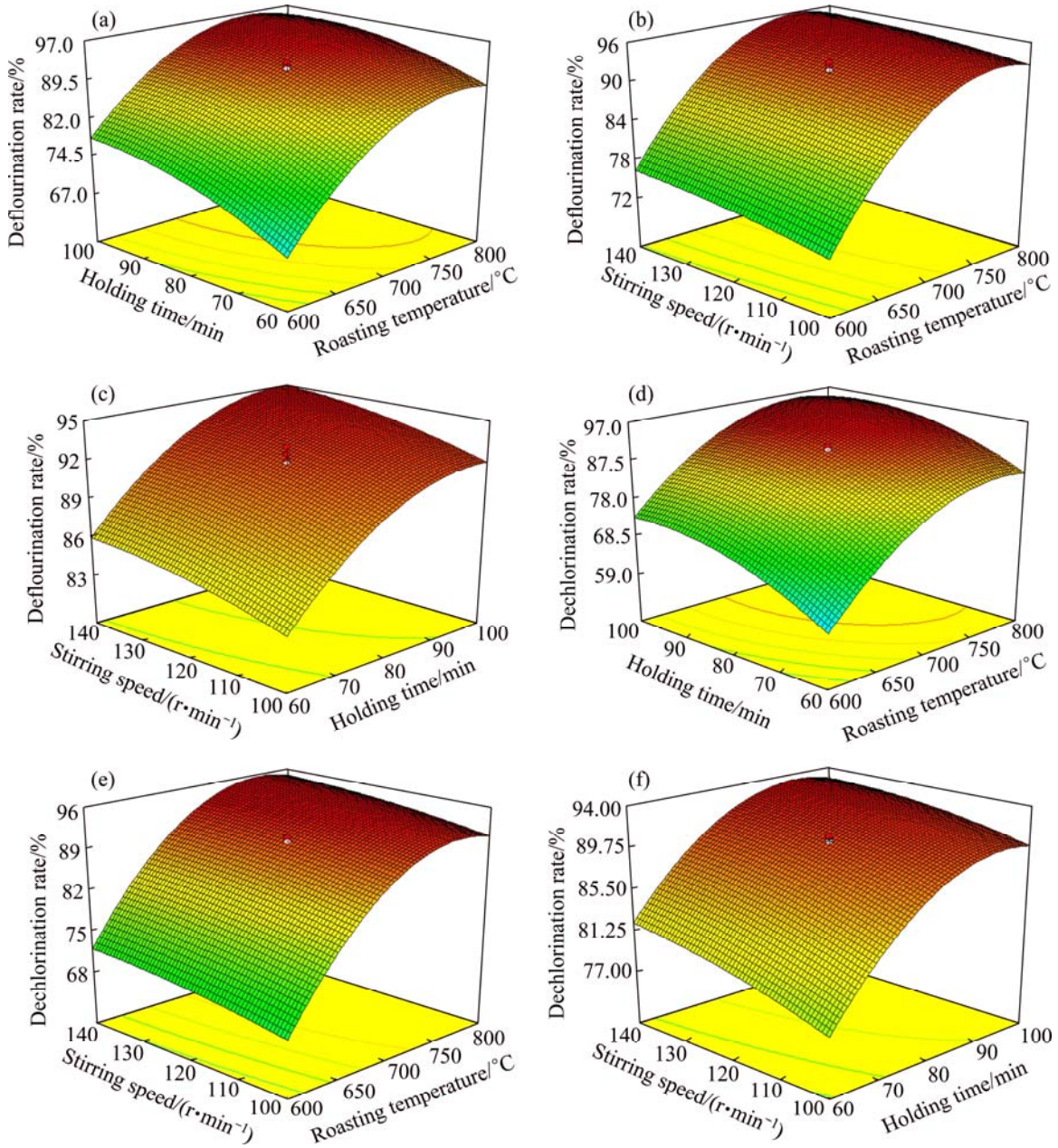

Fig. 4 Response surface plots of defluorination rate for roasting temperature vs holding time (a), roasting temperature vs stirring speed (b), holding time vs stirring speed (c), and response surface plots of dechlorination rate for roasting temperature vs holding time (d), roasting temperature vs stirring speed (e) and holding time vs stirring speed (f)

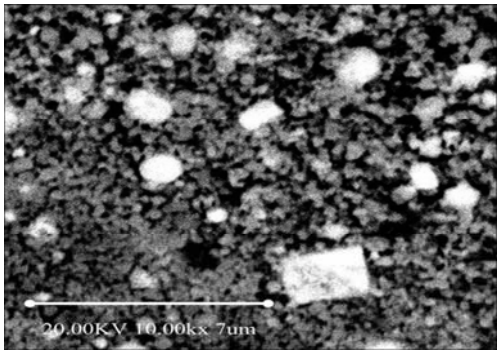

Fig. 5 SEM image of zinc oxide dust sample

with the extending of holding time. Compared with the stirring speed, the holding time had a more significant effect on the rate. The heating curves of 300 g zinc oxide fume under microwave power of 1200 W and 1800 W are plotted in Fig. 8. The zinc oxide fume in microwave field reaches 800 °C within 8 min, which provides evidence of the effectiveness of microwave roasting system for defluorination and dechlorination.

However, the rate increases slowly after a certain holding time and a lot of dusts running into the dust and gas absorbing system will bring a serious blockage when the stirring speed is too large and the holding time is too

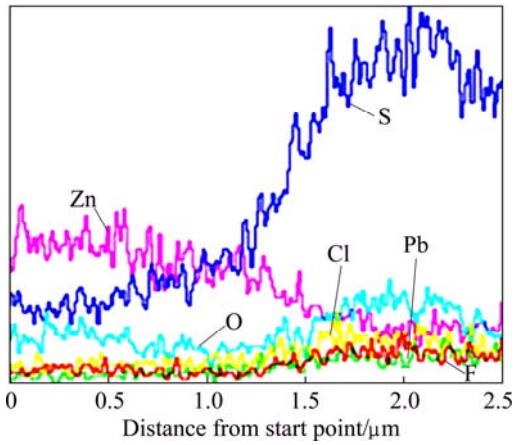

Fig. 6 EDS line scanning mapping of zinc oxide dust sample (from start to end of red line)

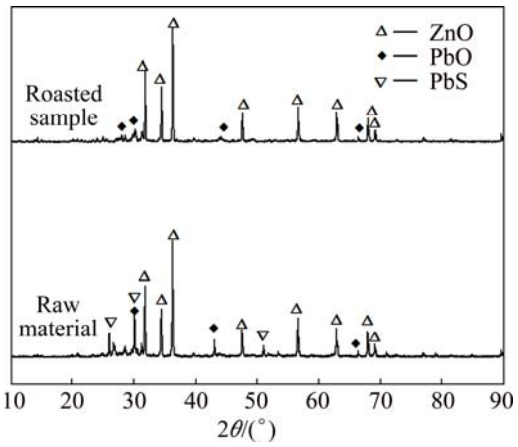

Fig. 7 XRD patterns of raw material and roasted sample

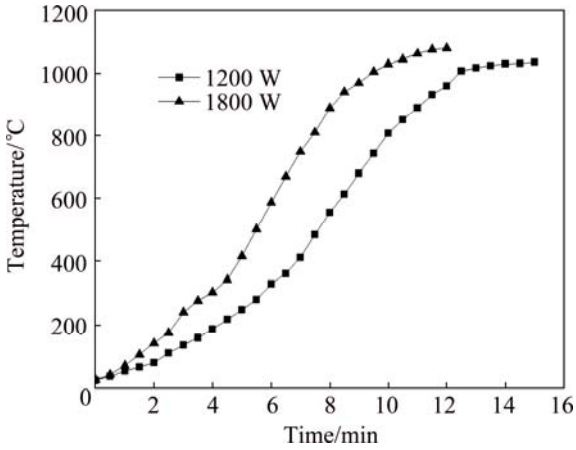

Fig. 8 Heating behavior of zinc oxide fumes at different microwave powers

long at the same point, which brings a significant effect on the dechlorination rate. Therefore, an appropriate factor is remarkable to control the impact on the defluorination and dechlorination rates.

3.3 Optimal conditions and verification of model

The aim of this study was to investigate the values of the three operational parameters (roasting temperature, holding time and stirring speed) that maximized the defluorination and dechlorination rates by using response surface methodology. The experimental values were compared with the predicted ones in order to determine the validity of the model.

From the model, optimized conditions were obtained and given in Table 6. The optimum levels of variables are found to be a roasting temperature of 700 °C, holding time of 80 min and stirring speed of 120 r/min with a prediction of 91.8% for the defluorination rate and a prediction of 90.5% for the dechlorination rate of zinc oxide dust. In order to test the validity of the optimum condition achieved by the empirical model, a confirmatory experiment was carried out using these optimal levels. The actual experimental value of defluorination rate is 92.6% and remains a relative error of 0.87% with the predicted value, while the actual experimental value of dechlorination rate is 90.2% and stays a relative error of 0.33% with the predicted value, which indicates that the experimental values are in agreement with the predicated ones. F and Cl contents of the roasted sample were measured to be 12.3 and 14.2 mg/L, respectively, satisfying the electrolysis requirements (ρ(F)<80 mg/L, ρ(Cl)<100 mg/L) in the zinc electrolysis process.

4 Conclusions

1) It is feasible to removal the fluorides and chlorides from zinc oxide dust obtained from fuming furnace by microwave roasting using response surface methodology.

2) The dechlorination rate of zinc oxide dust is significantly affected by roasting temperature and holding time compared with stirring speed.

3) The optimized roasting conditions are as follows: roasting temperature 700 °C, holding time 80 min and stirring speed 120 r/min. The defluorination and dechlorination rates of zinc oxide dust are 92.6% and 90.2%, respectively, which coincide well with

Table 6 Optimization process parameters of regression model

Roasting temperature, X_1/°C	Holding time, X_2/min	Stirring speed, X_3/(r·min^{-1})	Defluorination rate, Y_1/%		Dechlorination rate, Y_2/%	
			Predicted	Experimental	Predicted	Experimental
700	80	120	91.8	92.6	90.5	90.2

experimental values of 91.8% and 90.5% under the optimized conditions, suggesting that regressive equation fits the defluorination and dechlorination rates perfectly.

4) F and Cl contents of the roasted samples are removed to 12.3 and 14.2 mg/L, respectively, satisfying the electrolysis requirements in the zinc electrolysis process.

References

[1] LI Mi, PENG Bing, CHAI Li-yuan, PENG Ning, XIE Xian-de, YAN Huan. Technological mineralogy and environmental activity of zinc leaching residue from zinc hydrometallurgical process [J]. Transactions of Nonferrous Metals Society of China, 2013, 23(5): 1480−1488.

[2] MIN Xiao-bo, XIE Xian-de, CHAI Li-yuan, LIANG Yan-jie, LI Mi, KE Yong. Environmental availability and ecological risk assessment of heavy metals in zinc leaching residue [J]. Transactions of Nonferrous Metals Society of China, 2013, 23(1): 208−218.

[3] LI Xuan-hai, ZHANG Yan-juan, QIN Quan-lun, YANG Jian, WEI Yan-song. Indium recovery from zinc oxide flue dust by oxidative pressure leaching [J]. Transactions of Nonferrous Metals Society of China, 2010, 20(S): s141−s145.

[4] JHA M K, KUMAR V, SINGH R J. Review of hydrometallurgical recovery of zinc from industrial wastes [J]. Resource, Conservation & Recycling, 2001, 33(1): 1−22.

[5] IVANOV I, STEFANOV Y, NONCHEVA Z, PETROVA M, DOBREV T, MIRKOVA L, VERMEERSCH R, DEMAEREL J P. Insoluble anodes used in hydrometallurgy: Part I. Corrosion resistance of lead and lead alloy anodes [J]. Hydrometallurgy, 2000, 57(2): 109−124.

[6] LIU Qing, YANG Sheng-hai, CHEN Yong-ming, HE Jiang, XUE Hao-tian. Selective recovery of lead from zinc oxide dust with alkaline Na_2EDTA solution [J]. Transactions of Nonferrous Metals Society of China, 2014, 24(4): 1179−1186.

[7] CINAR SAHIN F, DERIN B, YÜCEL O. Chloride removal from zinc ash [J]. Scandinavian Journal of Metallurgy, 2000, 29(5): 224−230.

[8] LAN Y Z, ZHAO Q R, SMITH R W. Recovery of zinc from high fluorine bearing zinc oxide ore [J]. Mineral Processing and Extractive Metallurgy, 2006, 115(2): 117−119.

[9] WANG Ming-hui, WEI Li-qing, GUO Tian-li. Process study on removing chlorine from zinc oxide materials [J]. Non-ferrous Mining and Metallurgy, 2012, 28(4): 26−28. (in Chinese)

[10] CHEN W S, SHEN Y W, TSAI M S, CHANG F C. Removal of chloride from electric arc furnace dust [J]. Journal of Hazardous Materials, 2011, 190(1−3): 639−644.

[11] AL-HARAHSHEH M, KINGMAN S W. Microwave-assisted leaching—A review [J]. Hydrometallurgy, 2004, 73(3−4): 189−203.

[12] GUO Sheng-hui, CHEN Guo, PENG Jin-hui, CHEN Jin, LI Dong-bo, LIU Li-jun. Microwave assisted grinding of ilmenite ore [J]. Transactions of Nonferrous Metals Society of China, 2011, 21(9): 2122−2126.

[13] LI Yu, LEI Yin, ZHANG Li-bo, PENG Jin-hui, LI Chang-long. Microwave drying characteristics and kinetics of ilmentile [J]. Transactions of Nonferrous Metals Society of China, 2011, 21(1): 202−207.

[14] LIU Shu-zhen, BAI Yan, CHENG Yan-min, ZHONG Wen. Application of microwave technology in metallurgy [J]. Hydrometallurgy of China, 2001, 30(2): 91−96. (in Chinese)

[15] HAQUE K E. Microwave energy for mineral treatment processes—A brief review [J]. International Journal of Mineral Processing, 1997, 57(1): 1−24.

[16] PENG Jin-hui, YANG Xian-wan. The new applications of microwave power [M]. Kunming: Yunnan Science and Technology Press, 1997. (in Chinese)

[17] SUN Z, STEVEN J, WEN X, D'HEILLY J Y. Fluoride ion selective electrode: United States, US 2007/0199816 A1 [P]. 2007−08−30.

[18] ZENKI M, IWADOU Y. Repetitive determination of chloride using the circulation of the reagent solution in closed flow-through system [J]. Talanta, 2002, 58(6): 1055−1061.

[19] MYERS R H, MONTGOMERY D C, ADWESON-COOK C M. Response surface methodology: Process and product optimization using designed experiments [M]. New York: John Wiley and Sons, Inc, 2008.

[20] YANG Ke-di, YE Xian-jin, SU Jing, SU Hai-feng, LONG Yun-fei, LÜ Xiao-yan, WEN Yan-xuan. Response surface optimization of process parameters for reduction roasting of low-grade pyrolusite by bagasse [J]. Transactions of Nonferrous Metals Society of China, 2013, 23(2): 548−555.

响应面法优化微波焙烧氧化锌烟尘脱氟、氯工艺参数

李志强[1,2,3,4,5]，李 静[1,2,3,4,5]，张利波[1,2,3,4,5]，彭金辉[1,2,3,4,5]，王仕兴[1,2,3,4,5]，马爱元[1,2,3,4,5]，王宝宝[1,2,3,4,5]

1. 昆明理工大学 云南省特种冶金重点实验室，昆明 650093；
2. 昆明理工大学 微波能工程应用及装备技术国家地方联合工程实验室，昆明 650093；
3. 昆明理工大学 非常规冶金教育部重点实验室，昆明 650093；
4. 昆明理工大学 超硬材料先进制备技术国际联合研究中心，昆明 650093；
5. 昆明理工大学 冶金与能源工程学院，昆明 650093

摘 要：研究微波焙烧烟化炉产氧化锌烟尘脱除氟氯工艺，采用响应曲面法对焙烧温度、保温时间和搅拌速度三个重要工艺参数进行优化。结果表明：焙烧温度和保温时间对氟、氯脱除效果影响最显著，搅拌速度的次之；在焙烧温度为 700 ℃、保温时间为 80 min 和搅拌速度为 120 r/min 的条件下，氟和氯的脱除率分别达到 92.6%和 90.2%。上述结果表明，微波焙烧烟化炉产氧化锌烟尘脱氟氯工艺稳定可靠，效果显著。

关键词：氧化锌烟尘；氟；氯；脱除率；微波焙烧；响应曲面法

(Edited by Wei-ping CHEN)